

# Viscosity and solute dependence of F-actin translocation by rabbit skeletal heavy meromyosin

P. BRYANT CHASE,<sup>1,2</sup> YING CHEN,<sup>1</sup> KRISTI L. KULIN,<sup>3</sup> AND THOMAS L. DANIEL<sup>3</sup>  
Departments of <sup>1</sup>Radiology, <sup>2</sup>Physiology and Biophysics,  
and <sup>3</sup>Zoology, University of Washington, Seattle, Washington 98195

**Chase, P. Bryant, Ying Chen, Kristi L. Kulin, and Thomas L. Daniel.** Viscosity and solute dependence of F-actin translocation by rabbit skeletal heavy meromyosin. *Am J Physiol Cell Physiol* 278: C1088–C1098, 2000.—We tested the hypothesis that solvent viscosity affects translocation of rhodamine phalloidin-labeled F-actin by rabbit skeletal heavy meromyosin (HMM). When viscosity was increased using either glycerol, fructose, sucrose, or dextran (1.5, 6.0, or 15–20 kDa mol mass), there was little or no effect on the fraction of moving filaments, whereas sliding speed decreased in inverse proportion to viscosity. The results could be explained neither by an effect of osmotic pressure at high solute concentrations nor by altered solvent drag on the actin filament. Elevated viscosity inhibited HMM ATPase activity in solution, but only at much higher viscosities than were needed to reduce sliding speed. Polyethylene glycols (300, 1,000, or 3,000 mol wt) also inhibited speed via elevated viscosity but secondarily inhibited by enhancing electrostatic interactions. These results demonstrate that a diffusion-controlled process intrinsic to cross-bridge cycling can be limiting to actomyosin function.

in vitro motility assay; protein dynamics of biological motors; diffusion; sugars; polyethylene glycols

MYOSIN UTILIZES the free energy of ATP hydrolysis for translocation of actin filaments which, in muscle, results in sarcomere shortening. Such macroscopic motion in muscle contraction results from highly dynamic, microscopic motions of myosin's motor domain interacting with actin (27, 33, 44, 49). The factor that limits actin filament translocation by these dynamic motions of actomyosin at saturating, physiological ATP concentrations is a significant, unresolved question in the function of this molecular motor (3, 9, 22, 47, 51, 53).

Solvent viscosity affects dynamic motions of proteins (1, 25, 31), and, in general, the kinetics and energetics of macromolecular interactions that derive from thermal fluctuations (4, 23, 25, 28). Increased solvent viscosity slowed both the velocity of unloaded shortening ( $V_{US}$ ) and the rate of isometric tension redevelopment ( $k_{TR}$ ) of skinned muscle fibers at physiological [MgATP] and saturating [ $Ca^{2+}$ ] (7). Both kinetic parameters varied with the inverse of viscosity, implying a dependence on diffusion coefficient (4, 12). Viscous

resistance to filament sliding is not a significant factor because both isotonic ( $V_{US}$ ) and isometric ( $k_{TR}$ ) kinetics are affected equally by viscosity. The underlying limitation to  $V_{US}$  and  $k_{TR}$  at elevated viscosity could be diffusion of myosin heads to binding sites on actin or a subsequent step related to conformational changes in the actomyosin complex that results in isometric force generation and filament sliding.

As an initial step toward identifying the diffusion-controlled process that limits contraction kinetics, we used several classes of low-molecular-weight solutes to vary solvent viscosity in the in vitro motility assay. This assay provides a unique tie between biochemistry and physiology through quantifying motion of individual actin filaments. It has the benefit that it is in many ways simpler than a skinned muscle fiber. In the minimal motility assay, only the motor protein myosin [e.g., as heavy meromyosin (HMM)] is necessary for translocation of fluorescently labeled F-actin (29, 30).

A wide variety of solutes have been tested previously in actomyosin assays, but, in most instances, bulk viscosity of the solvent was not greatly altered. Two exceptions are methylcellulose (MC) and polyethylene glycol (PEG). MC lowers the probability that actin filaments dissociate from the HMM-coated surface in motility assays by restricting lateral but not axial motions (by diffusion and by directed transport) of actin filaments (14, 20, 21, 30, 36, 37, 46, 50, 51). Thus, MC has little effect, or, in some circumstances, increases sliding speed of F-actin. MC is large, however, relative to the proteins under study; therefore, it affects the macroscopic, but not the microscopic, viscosity that is more relevant to protein function (30). Low-molecular-weight PEGs do affect the microscopic viscosity, but have also been suggested to increase the affinity of myosin subfragment 1 (S1) for actin due to elevated osmotic pressure (18). Thus both of these solutes were considered as part of our study on viscosity and actomyosin function in the motility assay.

The results of this work demonstrate that low-molecular-weight solutes inhibit the sliding speed of F-actin in the in vitro motility assay by increasing solvent viscosity, indicating that this process can be diffusion limited. This diffusional limitation is intrinsic to actomyosin. Specific low-molecular-weight solutes (PEGs and possibly ethylene glycol) exhibited an additional mode of inhibition, enhancement of charge-charge interactions, that was overcome by increased

The costs of publication of this article were defrayed in part by the payment of page charges. The article must therefore be hereby marked "advertisement" in accordance with 18 U.S.C. Section 1734 solely to indicate this fact.

salt concentration. Portions of these results have appeared in abstract form (6, 8).

## METHODS

All aspects of motility experiments were performed and analyzed essentially as described previously (14, 45), with the exception of modifications to solutions. Brief details of the methods are given below.

### *Protein Preparations*

Myosin and F-actin were prepared from rabbit skeletal muscles according to Margossian and Lowey (34) and Pardee and Spudich (41), respectively. Chymotryptic digestion of myosin was used to prepare HMM (30). Concentrations of purified proteins were determined spectrophotometrically using the following extinction coefficients and molecular masses:  $0.53 \text{ cm}^{-1}$  (280 nm) and  $520 \text{ kDa}$  for myosin;  $0.6 \text{ cm}^{-1}$  (280 nm) and  $350 \text{ kDa}$  for HMM; and  $0.62 \text{ cm}^{-1}$  (290 nm) and  $42 \text{ kDa}$  for actin. At the beginning of each day of experiments, ATP-insensitive heads were removed from HMM by ultracentrifugation in the presence of unlabeled F-actin and MgATP (30); [HMM] was again determined subsequent to this procedure using the Bradford assay. Rhodamine phalloidin (RhPh; Molecular Probes, Eugene, OR) labeling of F-actin was accomplished according to Kron et al. (30).

All proteins were analyzed by SDS-PAGE, and both myosin and HMM were assayed for K-EDTA and  $\text{Ca}^{2+}$ -ATPase activities (14, 34, 45). In some experiments,  $\text{Mg}^{2+}$ -ATPase activity of HMM was also measured. ATPase reactions were initiated by addition of  $2.5 \text{ mM}$  ATP and terminated with SDS. ATPase activity was determined from the slope of  $\text{P}_i$  production (monitored colorimetrically) (52) vs. time after subtraction of background. Conditions for K-EDTA ATPase assays were:  $0.6 \text{ M}$  KCl,  $50 \text{ mM}$  Tris (pH 7.9),  $1 \text{ mM}$  EDTA, and  $0.1 \mu\text{M}$  myosin ( $0.2 \mu\text{M}$  S1). Conditions for  $\text{Ca}^{2+}$ -ATPase assays were:  $0.23 \text{ M}$  KCl,  $50 \text{ mM}$  Tris,  $2.5 \text{ mM}$   $\text{CaCl}_2$ , and  $0.2 \mu\text{M}$  myosin ( $0.4 \mu\text{M}$  S1). Conditions for  $\text{Mg}^{2+}$ -ATPase assays were:  $10 \text{ mM}$  imidazole (pH 7.9),  $2 \text{ mM}$   $\text{MgCl}_2$ ,  $0.1 \text{ mM}$   $\text{K}_2\text{EGTA}$ ,  $1 \text{ mM}$  dithiothreitol (DTT), and  $1.5 \mu\text{M}$  myosin ( $3 \mu\text{M}$  S1). All assays were carried out at  $23^\circ\text{C}$ . For myosin, K-EDTAATPase activity was  $17.0 \pm 1.3 \text{ s}^{-1} \cdot \text{S1}^{-1}$  (mean  $\pm$  SD;  $N = 8$ ) and  $\text{Ca}^{2+}$ -ATPase activity was  $4.3 \pm 0.5 \text{ s}^{-1} \cdot \text{S1}^{-1}$  (mean  $\pm$  SD;  $N = 8$ ). In these experiments, 17 preparations of HMM were used, and the K-EDTA and  $\text{Ca}^{2+}$ -ATPase activities of a subset of four of these preparations were  $14.2 \pm 2.1 \text{ s}^{-1} \cdot \text{S1}^{-1}$  and  $4.0 \pm 0.8 \text{ s}^{-1} \cdot \text{S1}^{-1}$  (mean  $\pm$  SD), respectively.

### *In Vitro Motility Assays*

**Solutions.** All motility assays were accomplished in actin buffer (AB:  $25 \text{ mM}$  KCl,  $25 \text{ mM}$  imidazole,  $4 \text{ mM}$   $\text{MgCl}_2$ ,  $1 \text{ mM}$  EGTA,  $1 \text{ mM}$  DTT, pH 7.4) with nonionic solutes added as indicated in each experiment. Immediately before the motility assay,  $2 \text{ mM}$  ATP,  $16.7 \text{ mM}$  glucose,  $100 \mu\text{g/ml}$  glucose oxidase,  $18 \mu\text{g/ml}$  catalase, and an additional  $40 \text{ mM}$  DTT were added to AB. The latter agents minimize photobleaching of the fluorescent label and photooxidative damage to the proteins (14, 30). In a limited subset of experiments, additional KCl or potassium acetate was added to increase ionic strength ( $\Gamma/2$ ). Except where indicated, MC was not added to motility buffers in these experiments because actin filaments did not dissociate from the flow cell surface under most conditions studied. In addition, MC adds significantly to the macroscopic viscosity of motility buffers, whereas, due to its large size relative to myosin, actin, and the other solutes studied, it adds little to the microscopic viscosity, i.e., the effective viscosity relevant at the size scale of myosin and the

diameter of actin filaments (30, also see RESULTS). The flow cell temperature was maintained at  $30^\circ\text{C}$  by temperature-controlled water circulated through a copper coil on the microscope objective (14, 25).

The additional solutes used in motility buffers were: fructose ( $180.16 \text{ mol wt}$ ; Sigma, St. Louis, MO); sucrose ( $342.3 \text{ mol wt}$ ; Pfanstiehl, Waukegan, IL; Boehringer-Mannheim, Indianapolis, IN); dextran ( $1.5, 6.0,$  and  $15\text{--}20 \text{ kDa}$  mol mass; Fluka, Ronkonkoma, NY); glycerol ( $92.11 \text{ mol wt}$ ; J. T. Baker, Phillipsburg, NJ); ethylene glycol ( $62.07 \text{ mol wt}$ ; Sigma); and polyethylene glycols ( $300, 1,000,$  and  $3,000 \text{ mol wt}$ ; Fluka). Motility buffers containing these various solutes were made in one of two ways. Either the solutes were dissolved directly in AB and the resulting volume changes measured to obtain the correct concentration, or (in most instances) motility buffers were made by mixing appropriate volumes of concentrated stock solutions plus water to obtain the correct final dilution; no significant differences were noted between results obtained using these two methods where direct comparisons were made.

Vapor pressure osmometry (model 5500; Westcor, Logan, UT) was used to verify osmolarity of motility buffers up to  $\sim 1,000 \text{ mosmol/kgH}_2\text{O}$ , the upper limit of the instrument. The osmolarity of motility buffer (AB with glucose, glucose oxidase, catalase, and DTT added) was  $187 \pm 5 \text{ mosmol/kgH}_2\text{O}$  (mean  $\pm$  SD;  $N = 13$ ).

Relative viscosity ( $\eta/\eta_0$ ) of solutions made in AB (without antibleaching agents) was determined (relative to the viscosity of deionized water,  $\eta_0$ ) using an Ostwald-type viscometer (VWR Scientific, West Chester, PA) and measured solution density (7, 35). The viscometer was held in a temperature-regulated water bath maintained at  $30^\circ\text{C}$ , the experimental temperature. After  $\eta/\eta_0$  was determined for solute concentrations over the range used in motility experiments, the results for each solute were fit to the function

$$\frac{\eta([\text{solute}])}{\eta_0} = A[\text{solute}]^B + \frac{\eta(0)}{\eta_0}$$

using nonlinear least-squares regression to obtain estimates of the regression parameters  $A$  and  $B$  (7). The relative viscosity for AB with no added solutes [ $\eta(0)/\eta_0$ ] was constrained to be equal to the average of measured values ( $1.018 \pm 0.014$ ; mean  $\pm$  SD;  $N = 7$ ).

**Flow cells.** To construct flow cells, no. 1 glass coverslips were coated with a thin layer of  $0.1\%$  nitrocellulose in amyl acetate (Ernest Fullam, Latham, NY), dried, and mounted on untreated microscope slides with no.  $1\frac{1}{2}$  spacers using silicone high-vacuum grease (30). Solutions were applied to the flow cell at room temperature in the order previously described (14). First, HMM was adsorbed to the flow cell surface at  $250 \mu\text{g/ml}$  in the majority of experiments, or, in a subset of experiments, at lower concentrations to reduce HMM density on the flow cell surface (13, 50, 51). For  $\text{HMM} \leq 100 \mu\text{g/ml}$ , HMM was diluted with AB + BSA (13). Application of HMM was followed by  $0.5 \text{ mg/ml}$  BSA in AB to block nonspecific protein binding and then AB alone to wash out unbound BSA. To inhibit actin binding by ATP-insensitive heads that either were not removed during preparation (see *Protein Preparations*) or were formed upon binding to the nitrocellulose-coated coverslip, short, unlabeled F-actin ( $0.1 \text{ mg/ml}$ , sheared by multiple, rapid passages through a 23-gauge needle) was applied to the flow cell. This was followed by  $0.5 \text{ mM}$  ATP in AB to dissociate the unlabeled F-actin from competent heads; a wash with AB solution was used after each of these steps to remove excess reagents. Diluted (1:100) RhPh F-actin (final concentration  $8 \text{ nM}$  actin monomer) was added to obtain a

suitable density (30), washed with AB to remove excess labeled filaments, and finally the motility buffer was infused into the flow cell.

**Microscopy.** After addition of the motility buffer, the flow cell was transferred to the stage of a Diastar upright fluorescence microscope (Leica, Deerfield, IL), and the flow cell was allowed to temperature equilibrate for  $\sim 1$  min (14, 24). Typically, six to eight fields (range 3–23) from various parts of the flow cell were imaged for  $\sim 1$  min each. Imaging was accomplished with a silicon intensifier target camera (model VE 1000; Dage-MTI, Michigan City, IN) and was recorded with an added time-date generator signal (model WJ-810; Panasonic, Secaucus, NJ) on VHS videocassettes (VCR model AG7350; Panasonic) for subsequent analysis (14).

#### Data Acquisition and Analysis

RhPh F-actin speed distributions were obtained by using hardware and Expert Vision software from Motion Analysis Systems (Santa Rosa, CA) (14, 20, 21, 46). In brief, centroids were calculated from filament outlines (obtained using hardware edge detection) that had been digitized at 10 frames/s (fps) for 20–60 s (typically 60 s). For a subset of the data, the Expert Vision software was programmed at this point to retain only those filaments within a specific size range for subsequent analysis. Speed statistics were calculated for each filament centroid that could be unambiguously tracked along its path for at least 2 s, and the ratio of SD to mean speed ( $r_U$ ) was calculated as an indicator of uniformity of motion (14, 20, 21, 46). A filament was considered to move uniformly if  $r_U < 0.5$  for 10 fps sampling (or if  $r_U < 0.3$  for 2 fps sampling; see below). The fraction of uniformly moving filaments ( $f_U$ ) was defined as proportion of filament paths meeting the criterion for uniform motion. The mean speed ( $s_U$ ) was calculated as the unweighted mean of mean speeds from those filament paths that met the criterion for uniform motion. To facilitate comparison between data obtained on different days,  $s_U$  was normalized to that obtained in control conditions (AB motility buffer with no additional solutes).

When  $s_U$  was  $< 5 \mu\text{m/s}$ , the centroid position data were further processed to reduce the contribution of spurious, apparent high-speed measurements that resulted from pixel jitter in the edge detection hardware. First, the centroid position vs. time data in each filament path were smoothed using a five-point moving average filter (equal weights). Then, a subset of the data was retained to yield an effective sampling rate of 2 fps (14). To complete the analysis of smoothed data, further processing was as described above for unsmoothed (10 fps) data, except the criterion for uniform motion was made more stringent ( $r_U < 0.3$  for 2 fps data).

**Statistical analyses.** Summary statistics were obtained using Excel (version 7.0; Microsoft, Redmond, WA). Linear and nonlinear least-squares regression analyses were performed using SigmaPlot software (version 4.0; SPSS Science, Chicago, IL). An ANOVA model (SPLUS version 2000 software; MathSoft, Seattle, WA) was used to statistically examine the effects of HMM density and fructose concentration on both  $f_U$  and  $s_U$ . The model was in the form of a second order orthogonal polynomial that measures the independent effects of HMM density and [fructose] as well as their possible interactions. Statistical significance was accepted at the  $P < 0.05$  level.

## RESULTS

The mean speed obtained in control conditions (AB motility buffer) was  $5.85 \pm 1.30 \mu\text{m/s}$  (mean  $\pm$  SD), determined from the mean speed obtained in 61 flow

cells; this corresponds to a total of 71,782 filament paths (trajectories) examined, which in turn corresponds to  $> 2.6 \times 10^6$  individual speed determinations in control conditions alone. For the same control flow cells, the fraction of filaments moving uniformly ( $f_U$ ) was  $0.83 \pm 0.11$  (mean  $\pm$  SD).

#### Monosaccharides and Disaccharides

**F-actin motility.** When sucrose or fructose was added to motility buffers, the speed of RhPh F-actin movement slowed with little effect on the fraction of filaments moving uniformly (Figs. 1 and 2). In all but three out of 34 flow cells tested, a majority of filaments were identified as moving uniformly ( $f_U > 0.5$ ) at all concentrations of fructose or sucrose added (Fig. 1A), despite the significant depression of  $s_U$  (Figs. 1, B and C, and 2). The solute concentration dependence of  $s_U$  was different for fructose vs. sucrose (Fig. 1B), indicating that osmotic effects of these low-molecular-weight solutes are not responsible for inhibiting  $s_U$ . The speed data for sucrose and fructose converge, however, to a single function when solution viscosity is considered (Fig. 1C); note that in Fig. 1C and in other figures (Figs. 2, 5, 6B, 7B, 8B, and 9A), viscosity is plotted as  $(\eta/\eta_0)^{-1}$ , and, therefore, viscosity decreases from left to right along the abscissa.

A graded dependence of  $s_U$  upon  $(\eta/\eta_0)^{-1}$  with varied amounts of added sucrose, yet with little effect on  $f_U$ , is evident in the frame-to-frame speed measurement histograms from individual flow cells shown in Fig. 2. All speed measurements were included in these histograms, not just those from uniformly moving filaments. Although the centroid of each histogram (that strongly influences  $s_U$ ) varies monotonically with  $(\eta/\eta_0)^{-1}$ , there is little change in the proportion of speed measurements in the lowest bin of each histogram (that strongly influences  $f_U$ ). The apparent height of the speed histograms in Fig. 2 covaries with  $\eta/\eta_0$ , although this is not meaningful because the area within each histogram is constant (normalized to 100%), as is the bin size ( $0.25 \mu\text{m/s}$ ); therefore, the tighter clustering and thus smaller deviation of speeds at high viscosity [low  $(\eta/\eta_0)^{-1}$ ] yields a higher amplitude for these normalized data. Figure 2 illustrates that the summary statistics (METHODS) accurately reflect overall speed distributions observed at widely varying viscosities.

To test the hypothesis that microscopic but not macroscopic viscosity (determined by the size of the solutes relative to the proteins of interest) is the relevant parameter in these experiments, we added 0.5% MC to some assays (open symbols in Fig. 1). In confirmation of previous reports (21, 50), MC did not inhibit control assays (no sucrose or fructose added), with the trend for  $s_U$  to be slightly faster with MC (open squares in Fig. 1). Similarly, there was no additional inhibitory effect of MC on  $s_U$  in the presence of sucrose or fructose (Fig. 1). Note that [solute] in the presence of MC was considered to be that of sucrose or fructose alone (Fig. 1, A and B, and also in Figs. 6A and 9, B-E) because 0.5% MC has little effect on solution osmolarity. It is important to note that  $(\eta/\eta_0)^{-1}$  was plotted as

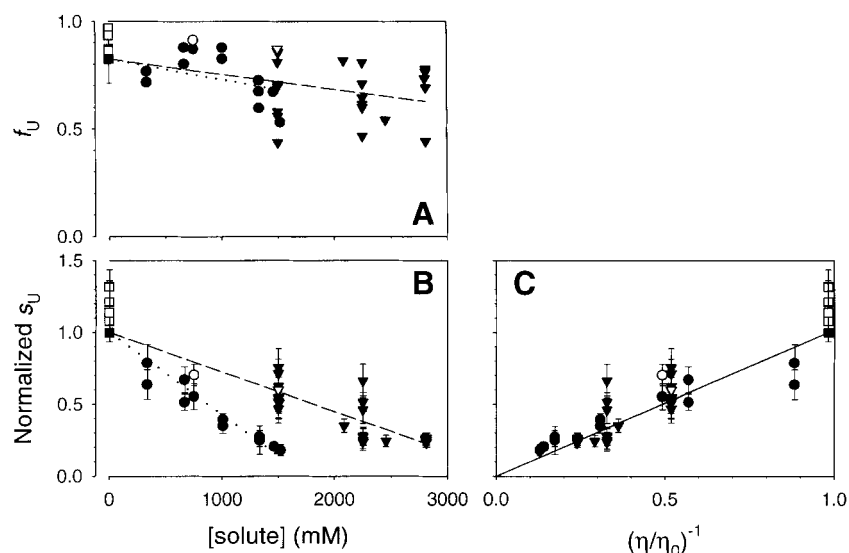


Fig. 1. Effect of fructose ( $\nabla$ ,  $\triangledown$ ) or sucrose ( $\bullet$ ,  $\circ$ ) on in vitro motility of rhodamine phalloidin (RhPh)-labeled F-actin. Motility assays were carried out using chymotryptic heavy meromyosin (HMM) on nitrocellulose-coated glass surfaces at 30°C (see METHODS). *A*: fraction of filaments moving uniformly ( $f_u$ ; see METHODS), and *B*: average speed of filaments moving uniformly ( $s_u$ ; see METHODS) as a function of [solute] added to motility buffer. *C*: dependence of  $s_u$  on inverse of solvent viscosity  $[(\eta/\eta_0)^{-1}]$ . In *B* and *C*,  $s_u$  was normalized to that obtained without added solute, and error bars are  $\pm 1$  SD. Data were obtained in absence ( $\nabla$ ,  $\bullet$ ,  $\blacksquare$ ) or presence ( $\triangledown$ ,  $\circ$ ,  $\square$ ) of 0.5% methylcellulose (MC). Note that for assays that included MC, only contributions of fructose and sucrose to added [solute] (*A* and *B*) and  $\eta/\eta_0$  (*C*) were plotted, and that neither contribution of MC to  $\eta/\eta_0$  nor minor contribution of MC to added [solute] was considered. Each point represents information from 1 flow cell, corresponding to  $1,570 \pm 680$  (fructose; mean  $\pm$  SD;  $n = 12$ ) or  $2,030 \pm 1,030$  (sucrose; mean  $\pm$  SD;  $n = 13$ ) filament paths. In *A* and *B*, lines are linear least-squares regressions constrained to pass through control values ( $\blacksquare$ ) for fructose (dashed line) or sucrose (dotted line). In *C*, solid line was drawn according to relationship for a diffusion-limited reaction.

that predicted for sucrose or fructose alone even though the measured (macroscopic) viscosity was increased ( $\sim 4$ - to 6-fold over AB) by MC (see also Ref. 50). Thus these data support the idea that the speed of actin

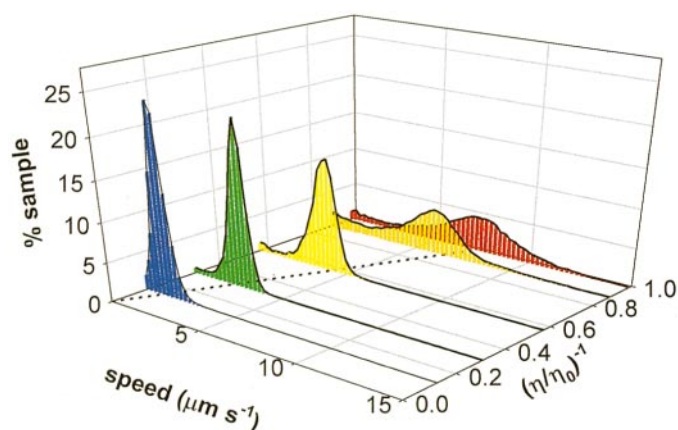


Fig. 2. Distributions of RhPh F-actin speed measurements at 330 mM (orange), 670 mM (yellow), 1,000 mM (green), and 1,500 mM (blue), or no (red) added sucrose. Each histogram corresponds to combined, frame-to-frame speed measurements from all filament paths of an individual flow cell. Number of observations and filament paths were: 52,494 and 2,170 (orange); 42,920 and 804 (yellow); 59,609 and 1,239 (green); 182,509 and 3,717 (blue); and 20,402 and 1,284 (red) before data smoothing (see METHODS; smoothing reduced number of observations in each path by 5-fold in yellow, green, and blue histograms only). Bin width was 0.25  $\mu\text{m/s}$ . Because total sample size was normalized to 100% for each condition, differences in maximum height are not meaningful. Dashed line in the  $x$ - $y$  plane was drawn according to relationship for a diffusion-limited reaction. Note smoothly graded slowing of entire speed histogram as viscosity ( $\eta/\eta_0$ ) was increased.

filament sliding is affected by microscopic viscosity of the buffer (i.e., the component of viscosity due to low-molecular-weight solutes, solutes that are small when compared with the proteins), but not necessarily the macroscopic viscosity.

The first possible mechanism to evaluate for retardation of filament sliding is viscous drag on the actin filament. This retarding force is proportional to both filament speed and length (16, 25). The calculated viscous drag force on an actin filament moving at maximal speed (including surface effects) is less than the force generated by a single cross bridge (38), in agreement with the conclusion from previous calculations (26). Thus viscous drag on a filament may not be significant compared with the net force of numerous cross-bridge interactions with each actin filament (of any length detectable in the fluorescence microscope) at saturating densities of HMM (METHODS and Ref. 51), or, increased numbers of force-generating interactions, assuming constant numbers of interactions per unit filament length, exactly balance the increase in viscous drag associated with increased filament length.

**Actin filament length.** In addition to model calculations, an experimental test is to examine speed as a function of filament length. We performed this analysis on a subset of data from eight flow cells, corresponding to a total of 9,085 filament paths; no normalization of speeds was used in this analysis because the data were compared within only a limited number of flow cells having similar mean speeds at each viscosity. In this subset of data,  $f_u$  was  $0.92 \pm 0.08$  (mean  $\pm$  SD;  $N = 9 =$

3 filament length distributions  $\times$  3 viscosities). Filaments of three size groups containing approximately equal numbers of filament paths were obtained by adjusting the Motion Analysis parameters (minimum and maximum number of pixels defining an object). If viscous drag was a significant factor, speed should decrease as filament length increases. Figure 3 shows that there was at most a small decrease in speed with filament length at the highest viscosity examined ( $\eta/\eta_0 = 3.9$ ), smaller than the order of magnitude range of filament lengths. No significant trend was observed either in the control condition, which agrees with previous reports under comparable conditions (50), or at an intermediate viscosity ( $\eta/\eta_0 = 2.5$ ).

**F-actin motility at reduced HMM density.** The results in Fig. 3 might be explained if the filament length-dependent change in retarding force (viscous drag) was exactly overcome by the change in total cross-bridge force due to a constant number of actomyosin interactions per unit length of the actin filament. To experimentally vary the number of cross bridges per micrometer of actin, density of HMM on the flow cell surface was altered in three separate experiments by varying the concentration of HMM applied (METHODS and Refs. 13, 50, 51). Motility was examined with either 0, 1.5, or 2.25 M fructose added. Both  $s_U$  (Fig. 4) and  $f_U$  decreased when HMM density was reduced sufficiently in the absence of added solutes. As shown for saturating HMM density in Fig. 1A, viscosity had little influence on  $f_U$  at any HMM density tested. Also, as demonstrated for saturating HMM (Fig. 1C), elevated viscosity inhibited  $s_U$  at all HMM densities studied (Fig. 4). Renormalization of the  $s_U$  data to that obtained at the same HMM density in the absence of fructose showed no systematic change in the effect of viscosity on  $s_U$  with HMM density. In particular, there was no significant enhancement of the viscosity effect at low-HMM density (ANOVA); if anything, elevated viscosity was less effective at inhibiting  $s_U$ . Taken together, the data in Figs. 3 and 4 demonstrate that viscous drag on the actin filament does not explain slowing of filament

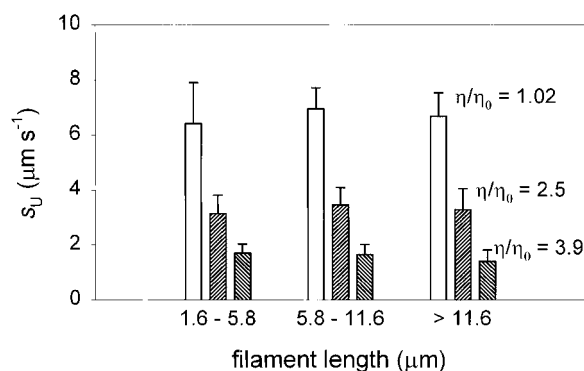


Fig. 3. Lack of dependence of RhPh F-actin speed on filament length at intermediate ( $\eta/\eta_0 = 2.5$ ), high ( $\eta/\eta_0 = 3.9$ ), and control ( $\eta/\eta_0 = 1.02$ ) viscosities. A total of 9,085 filament paths were examined from a subset of 8 flow cells from data shown in Fig. 1. Filament size bins were defined using Expert Vision/Motion Analysis system (see METHODS). These data indicate that speed is not significantly affected by viscous drag on actin filaments.

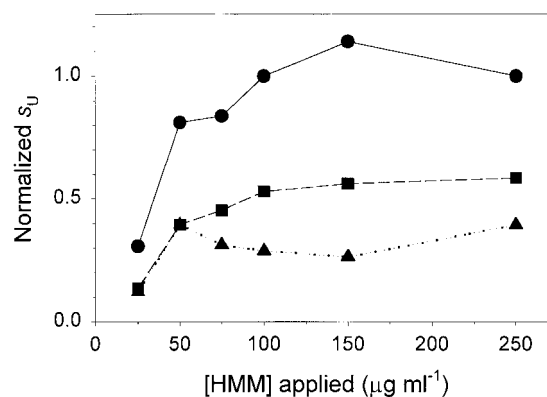


Fig. 4. Influence of elevated solvent viscosity on motility speed at reduced HMM density. HMM density of surface of flow cells was varied by changing concentration of HMM applied (METHODS). HMM density dependence of  $s_U$  at 1.5 M fructose ( $\blacksquare$ ; dashed lines), 2.25 M fructose ( $\blacktriangle$ ; dotted lines), or in absence of fructose ( $\bullet$ ; solid lines). All data were normalized to  $s_U$  obtained with 250  $\mu\text{g/ml}$  HMM in absence of fructose (obtained on same day) and each data point is average from 3 separate experimental days. Error bars omitted for clarity. Lines drawn to connect data points. Note that viscosity dependence of speed does not change in a graded manner with HMM density.

speed at elevated solution viscosities (Figs. 1–3), a conclusion consistent with data from skinned fibers (7). This suggests that viscosity acts on another aspect of F-actin translocation by HMM.

**HMM ATPase activity.** Because both fiber and motility assays indicated that solution drag is not a major determinant for actin filament sliding speed, we next tested for an effect of viscosity on diffusion of either substrate (MgATP) or products (MgADP,  $P_i$ , and  $H^+$ ) to/from the active site, or alternatively on domain motions that occur within myosin during the ATPase cycle.  $Ca^{2+}$ , K-EDTA, and  $Mg^{2+}$ -ATPase activities of HMM in solution were measured in the presence of 0–2.5 M sucrose.

In the absence of sucrose, K-EDTA ATPase activity was  $13.4 P_i S_1^{-1} \cdot s^{-1}$ ,  $Ca^{2+}$ -ATPase activity was  $4.0 P_i S_1^{-1} \cdot s^{-1}$ , and  $Mg^{2+}$ -ATPase activity was  $0.033 P_i S_1^{-1} \cdot s^{-1}$  (all values are the average from 2 experiments, each repeated in triplicate). The data in Fig. 5 were normalized to control measurements (no added sucrose) for direct comparison of viscosity effects on all three ATPase activities. As is evident in Fig. 5, the effect of elevated solvent viscosity on these three measures of HMM ATPase activities was evident only at viscosities much higher than necessary for slowing of  $s_U$  (Figs. 1C and 2; solid line in Fig. 5). The K-EDTA (closed circles) and  $Ca^{2+}$ -ATPases (closed triangles) were inhibited at the highest viscosities used [smallest  $(\eta/\eta_0)^{-1}$  in Fig. 5]. However, neither of these ATPase activities was significantly affected at intermediate viscosities (Fig. 5) where inhibition of  $s_U$  was clearly evident (Figs. 1 and 2). Similar results were obtained with myosin, although  $Mg^{2+}$ -ATPase activity of myosin was more inhibited than that of HMM at the highest viscosities tested (data not shown). These data indicate that the implied diffusional limitation to filament sliding is not related to an effect of viscosity on ATP hydrolysis by HMM.

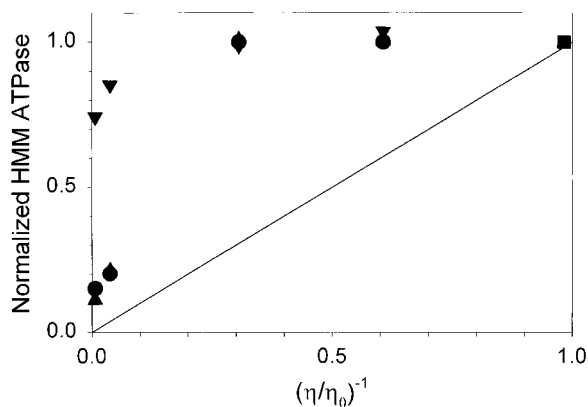


Fig. 5. Viscosity dependence of HMM K-EDTA ATPase (●), Ca<sup>2+</sup>-ATPase (▲), and Mg<sup>2+</sup>-ATPase (▼) activities in solution. ATPase activity was determined by measuring production of P<sub>i</sub> (see METHODS);  $\eta/\eta_0$  was varied by adding up to 2.5 M sucrose. All assays were performed in triplicate, and averaged ATPase activities were normalized to control measurements (■) obtained in absence of sucrose. Solid line was drawn according to relationship for a diffusion-limited reaction. Note that little or no effect of elevated viscosity on ATPase activity of HMM in solution was observed over a range of  $\eta/\eta_0$  that significantly inhibits F-actin sliding speed (Figs. 1–3).

*Polyethylene Glycols*

Because high concentrations of mono- and disaccharides were required to increase solution viscosity and inhibit F-actin sliding speed (Fig. 1), we performed assays with solutes other than mono- and disaccharides to test for a role of osmotic forces in the inhibition of  $s_U$ . We first tested polyethylene glycols (PEG 300, PEG 1,000, and PEG 3,000 mol wt). As shown in Fig. 6, all three PEGs strongly inhibited both  $s_U$  and  $f_U$ .

As was found for fructose and sucrose, inhibition by PEGs occurred over different concentration ranges that varied with solute size, with PEG 3,000 being effective at the lowest concentrations and PEG 300 at the highest concentrations. However, the effects of PEGs differed in many respects from the effects of fructose and sucrose. First, PEG 300 inhibited motility at lower concentrations than sucrose (compare closed hexagons in Fig. 6A with closed circles in Fig. 1, A and B) despite their similar mol wts (300 vs. 342.3), in contrast to the

expectation of the osmotic pressure hypothesis. Second, all three PEGs inhibited  $f_U$  (Fig. 6A) to a much greater extent than did sucrose or fructose (Fig. 1A). Motility stopped (Fig. 6), and the average length of actin filaments was shorter (data not shown) at the highest PEG concentrations, effects that were not observed with sucrose or fructose. Third, the inhibitory effects of PEG were greater than could be explained by an alteration of solution viscosity alone (Fig. 6B). Thus we concluded that PEGs inhibit actomyosin interactions via a mechanism beyond viscosity. This additional inhibitory activity could be related to osmotic pressure, as suggested by Highsmith et al. (18), although as mentioned above, the substantial differences between effects of sucrose and PEG 300 (despite the similarity of mol wt) argues against osmotic pressure being the pertinent variable.

*Ethylene Glycol and Glycerol*

Two additional commonly used reagents, ethylene glycol and glycerol, were also tested in the motility assay. In contrast to the PEGs tested (Fig. 6), which are substantially larger than fructose, both are smaller (mol wt 62.07 and 92.11, respectively) and thus we could more generally examine the possible roles of solvent viscosity and osmotic pressure and begin to examine the specific chemical nature of the solutes.

Both ethylene glycol and glycerol inhibited RhPh F-actin motility in a concentration-dependent manner, but concentrations of several molar were necessary to inhibit  $s_U$  by 50% or more (Fig. 7). There were differences in the inhibition by glycerol vs. ethylene glycol. Ethylene glycol (closed diamonds) had a greater effect on  $f_U$  than did glycerol (closed circles; Fig. 7A), although the effect of ethylene glycol on  $f_U$  was not as profound as that of PEGs (Fig. 6A). In addition, the effect of ethylene glycol on  $s_U$  (Fig. 7B) was similar to that of PEGs (Fig. 6B) insofar as it was greater than could be explained by a change in solution viscosity alone (solid lines in Figs. 6B and 7B). The complementary data with glycerol did not yield a clear answer on this point, although  $s_U$  varied with  $(\eta/\eta_0)^{-1}$  over most of the range studied (Fig. 7B). The data significantly diverged from

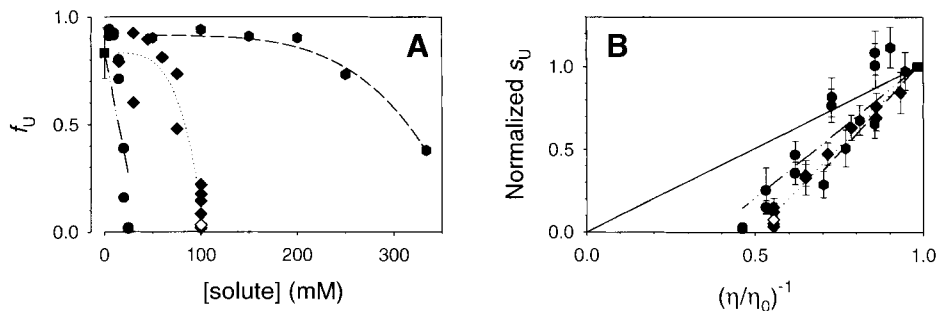
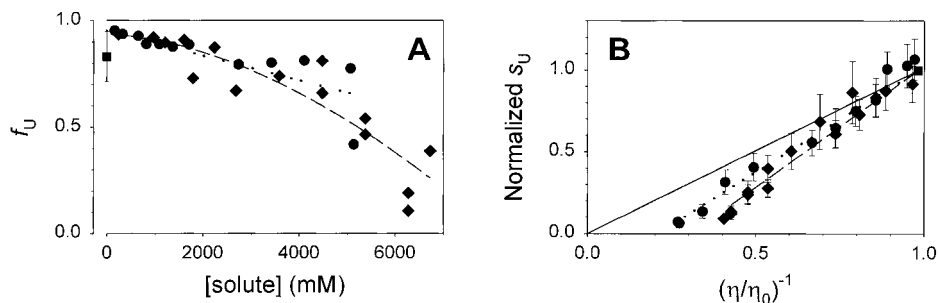


Fig. 6. Low-molecular-weight polyethylene glycols (PEGs) inhibit both (A)  $f_U$  and (B)  $s_U$  (see METHODS). Data were obtained with PEG 300 (closed hexagon; dashed lines), PEG 1,000 (◆; dotted lines), PEG 3,000 (●; dash-dotted lines), or in absence of PEG (■). Closed symbols indicate data obtained in absence of MC, whereas single open symbol indicates data obtained in presence of 0.5% MC (as in Fig. 1). Each point represents data summarized from a single flow cell, corresponding to  $2,100 \pm 980$  (PEG 300; mean  $\pm$  SD;  $N = 6$ ),  $2,080 \pm 1,230$  (PEG 1,000; mean  $\pm$  SD;  $N = 13$ ), and  $2,350 \pm 1,150$  (PEG 3,000; mean  $\pm$  SD;  $N = 10$ ) filament paths per flow cell. Note that  $f_U$  is significantly reduced in A and also that inhibition of  $s_U$  in B is greater than can be explained by a diffusional limitation of filament sliding (solid line).

Fig. 7. Inhibition of RhPh F-actin motility by ethylene glycol ( $\blacklozenge$ ; dashed lines) or glycerol ( $\bullet$ ; dotted lines). *A*: [solute] dependence of  $f_U$ ; *B*: dependence of  $s_U$  on inverse of relative viscosity  $[(\eta/\eta_0)^{-1}]$ . Control data are shown by  $\blacksquare$ . Each point represents data summarized from a single flow cell, corresponding to  $1,420 \pm 670$  (ethylene glycol; mean  $\pm$  SD;  $N = 16$ ) and  $1,520 \pm 660$  (glycerol; mean  $\pm$  SD;  $N = 12$ ) filament paths per flow cell. In *B*, solid line was drawn according to relationship for a diffusion-limited reaction.



the solid line in Fig. 7*B* only at the two highest glycerol concentrations; if this indicates an inhibitory effect of glycerol beyond that of elevated viscosity, it could be due to very high solute concentration (5 M). Thus the differences in ethylene glycol vs. glycerol effects on motility indicate that the latter acted more like fructose and sucrose (Figs. 1 and 2), whereas the former was more like its polymers, PEGs (Fig. 6), implicating the chemical nature of the solutes PEGs and possibly ethylene glycol (beyond viscous and osmotic forces) as being inhibitory for motility.

#### Dextrans

Given the evidence above that factors other than viscous and osmotic forces may be important for specific families of molecules (particularly PEGs in these studies), we chose to investigate the effects on motility of a second class of polymers of a range of mol wt that overlapped with our PEG studies shown in Fig. 6. Dextrans of 1.5, 6.0, and 15–20 kDa mol mass were used; the higher molecular mass dextran (15–20 kDa) was specifically chosen to address the question of whether a larger solute would be a more effective osmotic agent than smaller ones, being more readily excluded (e.g., Ref. 18).

Over the range of dextran concentrations tested,  $s_U$  decreased (Fig. 8*B*) with little or no effect on  $f_U$  for all three dextrans (Fig. 8*A*). Notably, the concentration ranges were similar to those in experiments with PEGs (Fig. 6). Most significant, the effect of dextran on  $s_U$  could be entirely explained by altered solution viscosity because  $s_U$  varied in proportion to  $(\eta/\eta_0)^{-1}$  (Fig. 8*B*), as

was found for fructose and sucrose (Figs. 1 and 2) and with glycerol (Fig. 7*B*), but unlike the results obtained with PEGs (Fig. 6*B*). These results strongly point toward solvent viscosity being an important factor in determining filament sliding speed, with some additional parameter being influential in the PEG experiments.

#### “Rescue” of Motility Inhibited by PEGs

To identify the extra parameter(s) of the motility assay, beyond viscosity, affected by PEGs (and possibly ethylene glycol, too), we tested for strengthening of ionic interactions between actin and myosin that could retard motion. The experimental design was to add to the motility buffer: 1) an amount of PEG that would significantly slow or stop motility (Fig. 6); plus 2) varying amounts of KCl above the nominal 25 mM in AB (METHODS), to increase  $\Gamma/2$ . The expectation of this experiment was that if the mechanism of PEG inhibition (Fig. 6) involves enhancement of ionic interactions, then both  $f_U$  and  $s_U$  should increase with added [KCl]; i.e., motility would be rescued by elevated  $\Gamma/2$ . Because PEG increases solvent viscosity,  $s_U$  was expected to be rescued not to control values but to the viscosity-limited value (thick solid line in Fig. 9*A*).

This prediction was tested with 7.5 or 10 wt% PEG 1,000 or 6 or 7.5 wt% PEG 3,000. Figure 9, *D* and *E*, shows results obtained in the presence of 10 wt% PEG 1,000, and illustrates that both  $f_U$  (Fig. 9*D*) and  $s_U$  (Fig. 9*E*) were rescued by addition of KCl; in a limited set of experiments, similar results were obtained with potassium acetate (closed hexagons in Fig. 9). Both param-

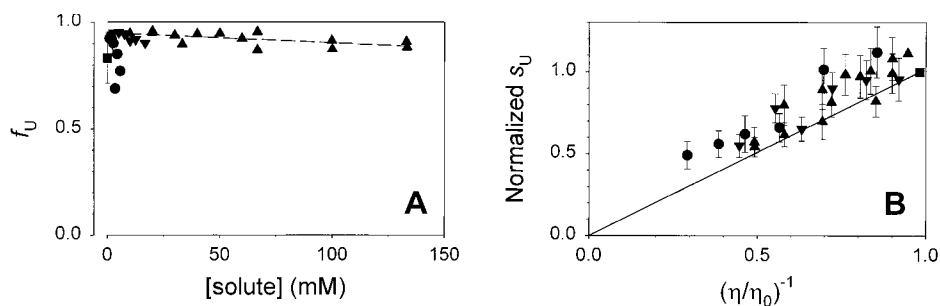


Fig. 8. Effects of dextran 1.5 kDa mol mass ( $\blacktriangle$ ; dashed line in *A*), dextran 6.0 kDa mol mass ( $\blacktriangledown$ ), and dextran 15–20 kDa mol mass ( $\bullet$ ) on motility of RhPh F-actin. Control data are shown by  $\blacksquare$ . Each point represents data summarized from a single flow cell, corresponding to  $1,750 \pm 540$  (dextran 1.5 kDa mol mass; mean  $\pm$  SD;  $N = 14$ ),  $2,380 \pm 420$  (dextran 6.0 kDa mol mass; mean  $\pm$  SD;  $N = 6$ ), and  $2,360 \pm 680$  (dextran 15–20 kDa mol mass; mean  $\pm$  SD;  $N = 6$ ) filament paths per flow cell. In *B*, the solid line was drawn according to relationship for a diffusion-limited reaction. Note similarities to data obtained with sucrose and fructose (Fig. 1), and differences from that with PEGs (Fig. 6).

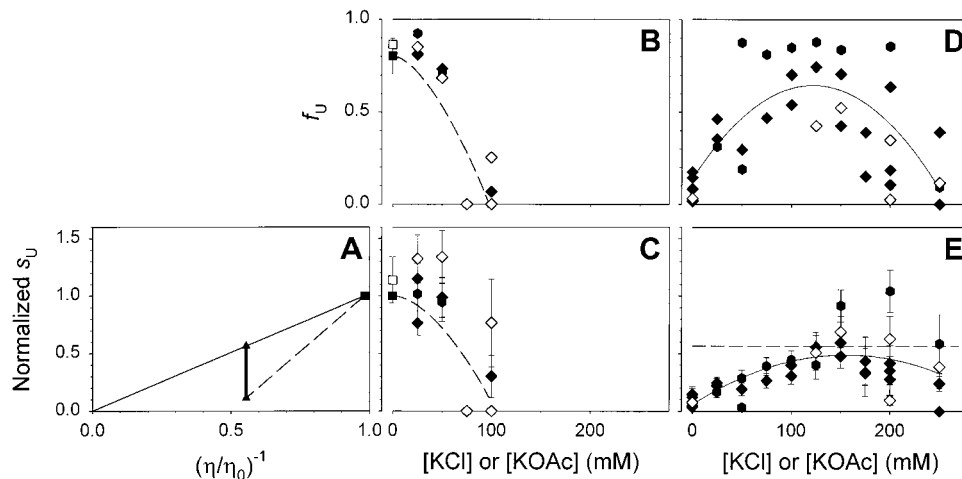


Fig. 9. Elevated ionic strength rescues RhPh F-actin motility inhibited by PEG. *A*: predicted rescue of RhPh F-actin  $s_U$ . Dashed line shows linear least-squares regression on PEG 1,000 data (Fig. 6*B*); thin solid line shows relationship for a diffusion-limited reaction. Thick solid line shows predicted increase of  $s_U$  in presence of 10 wt% PEG 1,000 to that of diffusional limitation. Data were obtained in absence (*B* and *C*) or presence (*D* and *E*) of 10 wt% PEG 1,000 and by adding either KCl ( $\blacklozenge$ ,  $\diamond$ ) or potassium acetate (closed hexagon). Abscissa in *B-D* indicates [KCl] or [potassium acetate] added to motility buffer, in addition to 25 mM KCl present in control assays ( $\blacksquare$ ,  $\square$ ). Data were obtained in absence ( $\blacklozenge$ , closed hexagon,  $\blacksquare$ ) or presence ( $\diamond$ ,  $\square$ ) of 0.5% MC. Solid lines in *D-E* are second order polynomial linear least-squares regressions on data. Dashed horizontal line in *E* is predicted, diffusion-limited speed at viscosity of 10 wt% PEG 1,000 (*A*). Note that at 100–150 mM added salt, little or no motility is observed in control assays (*B* and *C*) because filaments dissociate from HMM-coated surface (even in presence of 0.5% MC). In contrast, with 10 wt% PEG 1,000 in motility buffer, both  $f_U$  and  $s_U$  were substantially improved by 100–150 mM added salt (*D* and *E*).

eters varied biphasically with added KCl, exhibiting an optimum at 100–150 mM added salt. In the presence of 10 wt% PEG 1,000 and absence of added KCl (left-hand side of Fig. 9, *D* and *E*),  $f_U$  was low because filaments were bound to the surface but not moving or moving slowly and sporadically; some filament breakage was evident in this condition as described above, indicative of increased affinity between actin and HMM. Above the optimal [KCl],  $f_U$  decreased due to dissociation of F-actin from the HMM-coated surface, a phenomenon that is also observed at elevated  $\Gamma/2$  in the absence of PEGs (Fig. 9*B*) (21). A similar pattern was observed for  $s_U$  (Fig. 9*C*), although the decrease of  $s_U$  above optimal [KCl] is at least partially due to an inhibition of filament sliding on the surface of the flow cell rather than dissociation of filaments (21). At the optimal concentration of KCl,  $s_U$  was elevated to approximately that expected from elevated  $\eta/\eta_0$  ( $s_U$  57% of control; Fig. 9, *A* and *E*).

Results comparable to those shown in Fig. 9, *D* and *E*, for 10 wt% PEG 1,000 were also obtained with 7.5 wt% PEG 1,000 and 6 wt% PEG 3,000 (data not shown). This indicates that, at the minimum, PEGs exert two effects on F-actin translocation in the in vitro motility assay: elevated solvent viscosity and strengthening of ionic interactions. No rescue of motility was observed at 7.5 wt% PEG 3,000 for [KCl] up to 300 mM, which could be due to strongly enhanced ionic interactions, or to a secondary inhibition by such high [KCl] as suggested above. KCl rescue of motility inhibited by PEGs in three of the four conditions tested is taken as evidence against the possibility of a minor contaminant in each of the PEGs being the active inhibitory agent. The fact that rescue occurred by addition of KCl, i.e., an increase

in solution osmolarity, argues further against PEG affecting actomyosin interactions via osmotic pressure.

## DISCUSSION

The major findings of this study were: 1) sliding speed of RhPh F-actin on an HMM-coated surface varied in inverse proportion to the viscosity of the medium when low-molecular-weight solutes ( $\leq 20$  kDa) were used to alter viscosity, 2) the results could not be explained by an effect of osmotic pressure at high-solute concentrations, 3) slowing of filament sliding was not due to a viscous “load” or drag on F-actin, 4) elevated viscosity was not more effective at low densities of HMM on the flow cell surface, 5) elevated viscosity did not affect the HMM ATPase mechanism or diffusion of substrate or products to the same extent as sliding speed, and 6) polyethylene glycols inhibited in vitro motility by elevating solvent viscosity, but also exhibited a second inhibitory activity, i.e., strengthening of charge-charge interactions. Taken together, these results are consistent with filament sliding being limited by a diffusion-controlled process within the actomyosin cycle.

### *Does a Diffusion-Controlled Process Limit Functional Interactions of Actin and Myosin?*

The effect of adding either sucrose or fructose to the motility assay was comparable in many significant respects to results obtained with skinned fiber assays (7). The major finding, that speed was inversely proportional to  $(\eta/\eta_0)^{-1}$ , is consistent with some aspect of filament sliding kinetics being diffusion limited because of the implied linear dependence of rate on

diffusion coefficient (4, 12). The results from motility assays demonstrate that this effect does not involve the thin filament  $\text{Ca}^{2+}$ -regulatory proteins or additional sarcomeric proteins, and that the structural order of the sarcomere was not required for slower speeds at elevated  $\eta/\eta_0$ . All experiments were carried out at saturating levels of substrate because cross-bridge detachment could otherwise become limiting, particularly for filament sliding (9, 21). The fiber experiments demonstrated that these functional effects were readily reversible, indicating that protein structure was not drastically modified (e.g., denatured) by the solutes. High concentrations of added solutes affect a fundamental process underlying the kinetics of muscle contraction at the level of individual actin filaments, most likely via elevated viscosity.

To identify viscosity as the relevant parameter, it is necessary to eliminate the possibility of osmotic effects. We tested a variety of low-molecular-weight solutes and found that viscosity and not solute concentration influenced motility in the majority of solutes tested. The most notable exceptions were PEGs, which inhibited motility more than could be explained by viscosity alone (Fig. 6). PEGs had previously been suggested to increase the affinity of myosin for actin by increasing osmotic pressure (18), and the data in Fig. 6 could be consistent with such a mechanism. However, the effect of PEGs was overcome by adding KCl or potassium acetate (Fig. 9), which allowed us to conclude that the relevant secondary mechanism (beyond viscosity) was not osmotic but due to strengthening of ionic interactions. Figure 9 shows that PEG has two independent inhibitory effects on actomyosin function: one involving modulation of ionic interactions, and the other being elevation of solvent viscosity. Similar conclusions on the effect of PEGs on electrostatic interactions between proteins were also found in other studies on actin bundling (15) and aggregation of S1 (19). KCl also rescued motility inhibited by ethanol (17). Whether a similar mechanism is involved in inhibition by glycerol or ethylene glycol needs to be tested because earlier studies suggested that both compounds (at concentrations greater than the highest used in Fig. 7, and in the presence of nucleotide analogs rather than ATP) weakened the actomyosin bond (11, 42).

Related to the solvent viscosity dependence of a diffusion-controlled reaction is weak dependence on temperature (4, 12). The implication is that temperature's effect on rate arises from temperature-dependent changes in the viscosity of water ( $\eta_0$ ), therefore a  $Q_{10}$  in the range of 1.2–1.4 is expected. Maximum isometric force and several other contraction parameters meet this criterion (43), but force is not strongly dependent on viscosity (7). Both  $k_{\text{TR}}$  and unloaded sliding speed are typically reported to have  $Q_{10} > 1.5$  (5, 43). But, temperature dependence measured in intact preparations is complicated by  $\text{Ca}^{2+}$  release and uptake kinetics. In skinned fibers and motility assays, the temperature dependence of speed varies with salt concentration and with temperature itself, leaving the possibility that  $Q_{10}$ , at least at physiological temperature, is consistent

with diffusional limitation (2, 21). An additional complicating factor for interpreting temperature effects comes from changes in structure of the thick filament as temperature is varied (32). Therefore, temperature effects provide at best weak support for, but do not exclude, the argument that some aspect of actomyosin function is diffusion limited.

*What Is the Diffusion-Controlled Process That Limits Speed of Filament Sliding in the In Vitro Motility Assay and Contraction Kinetics in Skinned Muscle Fibers?*

Several factors beyond those outlined above can be eliminated as being diffusionally limited. First, the effect of viscosity was not due to a limitation of substrate diffusion or conformational changes during hydrolysis by HMM alone (Fig. 5). Second, fiber measurements (7), theoretical calculations (RESULTS and Refs. 25 and 26), and analysis of  $s_U$  vs. filament length (Fig. 5) all indicate that viscous retarding force does not limit actin filament sliding per se. Detailed analysis of data obtained at reduced motor density (e.g., Fig. 4) may be useful in distinguishing whether the attachment step (S1 diffusion to binding sites on actin) or molecular motions of the attached cross bridge are limiting. Theoretical considerations suggest that one would not expect to observe an effect of viscosity on attachment rates. As noted previously, the probability density function for the position of a cross bridge depends upon, among other factors, its spring constant and the temperature, but is independent of the fluid viscosity (10, 28, 40). This is because the thermal forcing of cross bridges depends linearly on their size and the viscosity of the medium. At the same time, the forces resisting their motion similarly are linearly dependent upon these parameters. Thus the size of the cross bridge and the viscosity of the medium cancel in equations that describe the probability density functions for their spatial location. Further, the mobility of spin-labeled myosin in fibers detected by electron paramagnetic resonance is found to change very little with viscosity of the medium (P. Fajer, personal communication).

The above arguments suggest that viscosity inhibits by influencing cross-bridge motions that occur after myosin binds to actin. Recent work shows that mobility of *loop 1* of S1, which modulates ADP release, is a candidate for the viscosity-sensitive step (39, 47, 48), although it is also plausible that viscosity directly affects motion associated with the cross-bridge powerstroke. Further experiments are required to identify the specific transitions affected. But clearly, viscosity is a useful tool for studying molecular motions of the cross bridge that underlie contractile function.

We thank D. Anderson, M. Bandy, D. Boster, J. Hawkins, M. Maker, M. Mathiason, B. Shepherd, R. Stefurak, and R. Yamamoto for excellent technical assistance; Drs. A. M. Gordon and M. A. LaMadrid for helpful suggestions; Dr. J. Nelson and L. Young for assistance with vapor pressure osmometry; Dr. P. Fajer for sharing preliminary EPR data; and Dr. J. G. Kingsolver for assistance with statistical analysis.

This work was supported by National Heart, Lung, and Blood Institute Grant HL-52558.

Address for reprint requests and other correspondence: P. B. Chase, Univ. of Washington, Depts. of Radiology and Physiology and Biophysics, Box 357115, Seattle, WA 98195-7115 (E-mail: chase@u.washington.edu).

Received 9 February 1999; accepted in final form 22 December 1999.

## REFERENCES

1. **Ansari A, Jones CM, Henry ER, Hofrichter J, and Eaton WA.** The role of solvent viscosity in the dynamics of protein conformational changes. *Science* 256: 1796–1798, 1992.
2. **Anson M.** Temperature dependence and Arrhenius activation energy of F-actin velocity generated in vitro by skeletal myosin. *J Mol Biol* 224: 1029–1038, 1992.
3. **Barman T, Brune M, Lionne C, Piroddi N, Poggesi C, Stehle R, Tesi C, Travers F, and Webb MR.** ATPase and shortening rates in frog fast skeletal myofibrils by time-resolved measurements of protein-bound and free P<sub>i</sub>. *Biophys J* 74: 3120–3130, 1998.
4. **Berg OG and von Hippel PH.** Diffusion-controlled macromolecular interactions. *Annu Rev Biophys Chem* 14: 131–160, 1985.
5. **Brenner B and Eisenberg E.** Rate of force generation in muscle: correlation with actomyosin ATPase activity in solution. *Proc Natl Acad Sci USA* 83: 3542–3546, 1986.
6. **Chase PB and Chen Y.** Inhibition of F-actin sliding speed in the in vitro motility assay by Dextran and polyethylene glycols (Abstract). *Biophys J* 74: A131, 1998.
7. **Chase PB, Denkinger TM, and Kushmerick MJ.** Effect of viscosity on mechanics of single, skinned fibers from rabbit psoas muscle. *Biophys J* 74: 1428–1438, 1998.
8. **Chase PB, Kulin K, and Daniel TL.** Slower in vitro motility of actin filaments with elevated solution viscosity (Abstract). *Biophys J* 72: A221, 1997.
9. **Chase PB and Kushmerick MJ.** Effect of physiological ADP levels on contraction of single skinned fibers from rabbit fast and slow muscles. *Am J Physiol Cell Physiol* 268: C480–C489, 1995.
10. **Daniel TL, Trimble AC, and Chase PB.** Compliant realignment of binding sites in muscle: transient behavior and mechanical tuning. *Biophys J* 74: 1611–1621, 1998.
11. **Fajer PG, Fajer EA, Brunsvold NJ, and Thomas DD.** Effects of AMPNP on the orientation and rotational dynamics of spin-labeled muscle cross-bridges. *Biophys J* 53: 513–524, 1988.
12. **Gabdouline RR and Wade RC.** Simulation of the diffusional association of barnase and barstar. *Biophys J* 72: 1917–1929, 1997.
13. **Gordon AM, Chen Y, Liang B, LaMadrid M, Luo Z, and Chase PB.** Skeletal muscle regulatory proteins enhance F-actin in vitro motility. *Adv Exp Med Biol* 453: 187–197, 1998.
14. **Gordon AM, LaMadrid M, Chen Y, Luo Z, and Chase PB.** Calcium regulation of skeletal muscle thin filament motility in vitro. *Biophys J* 72: 1295–1307, 1997.
15. **Goverman J, Schick LA, and Newman J.** The bundling of actin with polyethylene glycol 8000 in the presence and absence of gelsolin. *Biophys J* 71: 1485–1492, 1996.
16. **Happel JR and Brenner H.** *Low Reynolds Number Hydrodynamics*. Dordrecht, The Netherlands: Kluwer, 1981.
17. **Hatori K, Honda H, and Matsuno K.** ATP hydrolysis and sliding movement of actomyosin complex in the presence of ethanol. *J Biochem (Tokyo)* 117: 264–266, 1995.
18. **Highsmith S, Duignan K, Cooke R, and Cohen J.** Osmotic pressure probe of actin-myosin hydration changes during ATP hydrolysis. *Biophys J* 70: 2830–2837, 1996.
19. **Highsmith S, Duignan K, Franks-Skiba K, Polosukhina K, and Cooke R.** Reversible inactivation of myosin subfragment 1 activity by mechanical immobilization. *Biophys J* 74: 1465–1472, 1998.
20. **Homsher E, Kim B, Bobkova A, and Tobacman LS.** Calcium regulation of thin filament movement in an in vitro motility assay. *Biophys J* 70: 1881–1892, 1996.
21. **Homsher E, Wang F, and Sellers JR.** Factors affecting movement of F-actin filaments propelled by skeletal muscle heavy meromyosin. *Am J Physiol Cell Physiol* 262: C714–C723, 1992.
22. **Howard J.** Molecular motors: structural adaptations to cellular functions. *Nature* 389: 561–567, 1997.
23. **Howard J.** The movement of kinesin along microtubules. *Annu Rev Physiol* 58: 703–729, 1996.
24. **Howard J, Hunt AJ, and Baek S.** Assay of microtubule movement driven by single kinesin molecules. *Methods Cell Biol* 39: 137–147, 1993.
25. **Hunt AJ, Gittes F, and Howard J.** The force exerted by a single kinesin molecule against a viscous load. *Biophys J* 67: 766–781, 1994.
26. **Huxley A.** *Reflections on Muscle*. Princeton, New Jersey: Princeton Univ. Press, 1980.
27. **Huxley AF and Simmons RM.** Proposed mechanism of force generation in striated muscle. *Nature* 233: 533–538, 1971.
28. **Kramers HA.** Brownian motion in a field of force and the diffusion model of chemical reactions. *Physica* 7: 284–304, 1940.
29. **Kron SJ and Spudich JA.** Fluorescent actin filaments move on myosin fixed to a glass surface. *Proc Natl Acad Sci USA* 83: 6272–6276, 1986.
30. **Kron SJ, Toyoshima YY, Uyeda TQP, and Spudich JA.** Assays for actin sliding movement over myosin-coated surfaces. *Methods Enzymol* 196: 399–416, 1991.
31. **Kukita F.** Solvent-dependent rate-limiting steps in the conformational change of sodium channel gating in squid giant axon. *J Physiol (Lond)* 498: 109–133, 1997.
32. **Levine RJC, Kensler RW, Yang Z, Stull JT, and Sweeney HL.** Myosin light chain phosphorylation affects the structure of rabbit skeletal muscle thick filaments. *Biophys J* 71: 898–907, 1996.
33. **Lombardi V, Piazzesi G, Ferenczi MA, Thirwell H, Dobbie I, and Irving M.** Elastic distortion of myosin heads and repriming of the working stroke in muscle. *Nature* 374: 553–555, 1995.
34. **Margossian SS and Lowey S.** Preparation of myosin and its subfragments from rabbit skeletal muscle. *Methods Enzymol* 85: 55–71, 1982.
35. **McKie JE and Brandts JF.** High precision capillary viscometry. *Methods Enzymol* 26: 257–288, 1972.
36. **Miller CJ and Reisler E.** Role of charged amino acid pairs in subdomain-1 of actin in interactions with myosin. *Biochemistry* 34: 2694–2700, 1995.
37. **Miller CJ, Wong WW, Bobkova E, Rubenstein PA, and Reisler E.** Mutational analysis of the role of the N terminus of actin in actomyosin interactions. Comparison with other mutant actins and implications for the cross-bridge cycle. *Biochemistry* 35: 16557–16565, 1996.
38. **Molloy JE, Burns JE, Kendrick-Jones J, Tregear RT, and White DCS.** Movement and force produced by a single myosin head. *Nature* 378: 209–212, 1995.
39. **Murphy CT and Spudich JA.** *Dictyostelium* myosin 25–50K loop substitutions specifically affect ADP release rates. *Biochemistry* 37: 6738–6744, 1998.
40. **Papoulis A.** *Probability, Random Variables and Stochastic Processes*. New York: McGraw-Hill, 1991.
41. **Pardee JD and Spudich JA.** Purification of muscle actin. *Methods Enzymol* 85: 164–181, 1982.
42. **Pate E and Cooke R.** Energetics of the actomyosin bond in the filament array of muscle fibers. *Biophys J* 53: 561–573, 1988.
43. **Rall JA and Woledge RC.** Influence of temperature on mechanics and energetics of muscle contraction. *Am J Physiol Regulatory Integrative Comp Physiol* 259: R197–R203, 1990.
44. **Rayment I.** The structural basis of the myosin ATPase activity. *J Biol Chem* 271: 15850–15853, 1996.
45. **Regnier M, Martyn DA, and Chase PB.** Calmidazolium alters Ca<sup>2+</sup> regulation of tension redevelopment rate in skinned skeletal muscle. *Biophys J* 71: 2786–2794, 1996.
46. **Sellers JR, Cuda G, Wang F, and Homsher E.** Myosin-specific adaptations of the motility assay. *Methods Cell Biol* 39: 23–49, 1993.
47. **Siemankowski RF, Wiseman MO, and White HD.** ADP dissociation from actomyosin subfragment 1 is sufficiently slow to limit the unloaded shortening velocity in vertebrate muscle. *Proc Natl Acad Sci USA* 82: 658–662, 1985.

48. **Sweeney HL, Rosenfeld SS, Brown F, Faust L, Smith J, Xing J, Stein LA, and Sellers JR.** Kinetic tuning of myosin via a flexible loop adjacent to the nucleotide binding pocket. *J Biol Chem* 273: 6262–6270, 1998.
49. **Thomas DD, Ramachandran S, Roopnarine O, Hayden DW, and Ostap EM.** The mechanism of force generation in myosin: a disorder-to-order transition, coupled to internal structural changes. *Biophys J* 68: 135S–141S, 1995.
50. **Uyeda TQP, Kron SJ, and Spudich JA.** Myosin step size estimation from slow sliding movement of actin over low densities of heavy meromyosin. *J Mol Biol* 214: 699–710, 1990.
51. **Uyeda TQP, Warrick HM, Kron SJ, and Spudich JA.** Quantized velocities at low-myosin densities in an in vitro motility assay. *Nature* 352: 307–311, 1991.
52. **White HD.** Special instrumentation and techniques for kinetic studies of contractile systems. *Methods Enzymol* 85: 698–708, 1982.
53. **White HD, Belknap B, and Webb MR.** Kinetics of nucleoside triphosphate cleavage and phosphate release steps by associated rabbit skeletal actomyosin, measured using a novel fluorescent probe for phosphate. *Biochemistry* 36: 11828–11836, 1997.

